Final Report

EML4552C-Senior Design Spring 2014

Team 20- Direct Drive Solar-Powered Arcjet Thruster

Sponsor: Kurt Polzin (NASA)

Faculty Advisor: Wei Guo, Kwan Bing, Petru Andrei

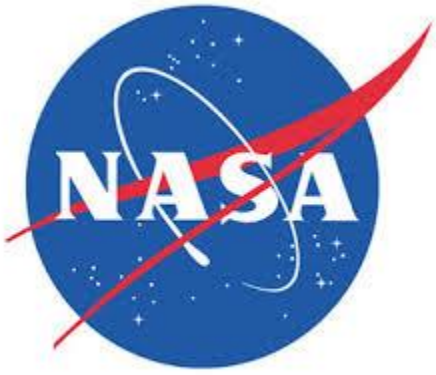

Group Members

Christopher Brolin

Cory Gainus

Gerard Melanson

Tara Newton

Griffin Valentich

Shane Warner

Table of Contents

1.0 Abstract

The importance of long term control of satellite and spacecraft systems provides an opportunity for advancement in existing propulsion technologies. For the scope of this project, a solar powered arcjet thruster must be designed that eliminates the necessity of a power processing unit (PPU). Currently, startup of the thruster is achieved by transforming solar power to a desirable voltage and current via the PPU. Lighter, more affordable arcjet systems can be sent into space if this PPU is eliminated and, instead, driven directly by the solar panels. This increases the efficiency of the thruster as one of the components that fails most often is the PPU as a result of overheating. One topic under examination is the amount of thrust that can be generated without this PPU, in so-called "direct drive mode". Reduced cost of a system that provides low thrust but high specific impulse in this manner could greatly improve the functionality of thrusters used in space.

2.0 Acknowledgements

Thanks to K. Polzin, W. Guo, J. Phillips, J. Gillman, K. Larson, M. Weatherspoon, and J. Zheng for their help and advice on this project.

3.0 Project Overview

3.1 Customer/Sponsor Requirements:

- Produce a high voltage-pulse that can breakdown the injected gas to cause ionization.
- Design a scalable arcjet thruster capable of processing a maximum of 400W of power without the use of a power processing unit.
- Design a vacuum chamber in order to properly simulate the space environment for testing the thruster.
- Design and execute a test/experiment in order to determine the thruster's range of operating conditions over which the ionization or gas breakdown will occur.
- Perform a successful test to quantify the conditions over which a continuous discharge at the given power levels can be sustained.
- Determine if this continuous discharge is possible within the range of conditions provided by the solar panels

3.2 Scope:

The project scope is to design, fabricate, and test an electric arcjet thruster within a vacuum chamber that will be designed to simulate the space environment at which the thruster will operate. The arcjet thruster will operate on a direct drive system eliminating the need for a power processing unit (PPU), thereby reducing the weight of the system, its complexity, and most importantly cost while maintaining efficiency. The use of solar panels as the arcjet's source of energy will be used since an abundance of solar energy is present in the space environment.

3.3 Goal:

To successfully design and test an arcject thruster within a vacuum chamber that meets all of our customer's requirements.

3.4 Objectives:

- Operate on direct drive by eliminating the PPU
- Generate an arc capable of breaking down a gas propellant
- Produce a current density that will sustain the plasma
- Produce a model that is scalable for NASA applications
- Design and build a reliable test model
- Create a space-like test environment
- Create and carry out an experiment to determine the amount of thrust produced

3.5 Constraints:

- Work within our budget of $500
- Time constraints of deliverables
- Minimize weight
- Set input power source (Solar arrays provided by NASA)
- Produce a pressurized gas within a vacuum environment

4.0 Design and Analysis

4.1 Functional Analysis

4.1.1 Mechanical

Gas Valve Regulator

The gas valve regulator will be provided by the manufacturer of the argon gas tank and will function as a control valve to regulate the flow of argon gas into the thruster.

Thruster Housing

The thruster housing will function as the body of the thruster which houses some of the major components such as the annular anode, cathode, and magnets. The housing will also function as a control volume by containing the argon gas in order to allow for the plasma to be created.

Anode/Cathode Spacing

The anode and cathode spacing within the thruster housing will function as a major component in the arcjet thruster. The spacing between the anode and cathode is important because it determines the breakdown voltage needed to ionize the argon gas.

Nozzle

The converging-diverging nozzle within the arcjet thruster will allow the argon ions generated by the arc to be accelerated past sonic velocity. The nozzle will also function with the help of magnets to contain the plasma at a centerline off the walls of the nozzle.

Vacuum Chamber

The vacuum chamber will be used to house the arcjet thruster in order to conduct a proper experiment simulating the space environment, where the arcjet thruster will be used.

4.1.2 Electrical

Circuit

The circuit will consist of solar panels, an inductor, an IGBT, pulse generator, and a potentiometer. The solar panels will provide electrical energy to the circuit and ionization process. The circuit must be capable of producing a voltage spike ranging from 137 V to 1.034 kV. Once the system is in steady state the current through the plasma (anode/cathode) should be approximately 5.5 A.

Magnets

The magnet is needed to direct flow of the plasma through the nozzle, protect the thruster from overheating, and help produce additional thrust.

4.2 Design Concepts

4.2.1 Mechanical

Design #1

The first design considered for this project was the baseline design produced by former NASA intern Nicholas Rongione. A schematic of this design is shown in Figure 1.

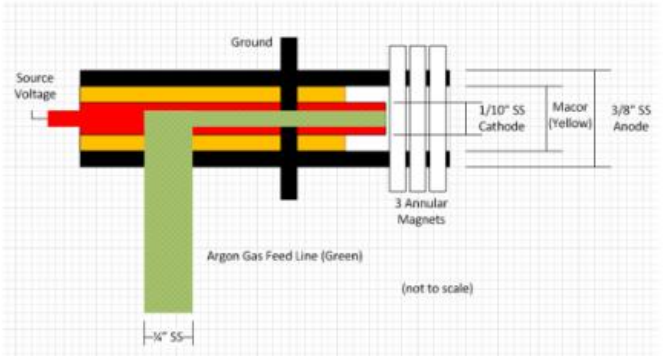

Figure 1: Mechanical Design 1

This design is characterized by a large cylindrical stainless steel tube acting as the anode, with a smaller stainless tube acting as the cathode. Both are along the same centerline axis. The argon gas enters into the housing and is injected directly into the cathode. The gas exits the cathode into a constant area nozzle surrounded by three annular magnets that directs the flow of the argon ions out of the nozzle, and protect the nozzle/anode walls from the high temperature fluid. The cathode is also insulated with Macor to prevent a short of the circuit.

Design #2

The next design improves upon Design 1 in that it utilizes a converging-diverging nozzle in order to help accelerate the flow of the argon gas passed sonic velocity. Rather than injecting the argon gas directly through the cathode, this design injects the gas into the thruster housing perpendicular to the cathode. This design concept is depicted in Figure 2.

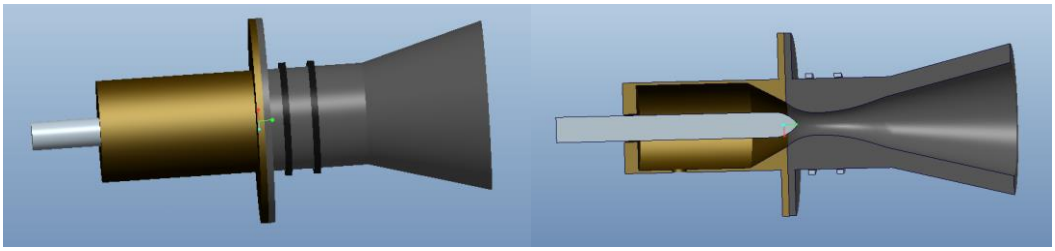

Figure 2: Mechanical Design 2

The converging diverging nozzle acts as the anode and the cylindrical rod with a pointed tip acts as the cathode. The magnets are placed around the front side of the nozzle and are represented as the rings in Fig. 2. The placement of the magnets will help confine the high temperature argon ions away from the surface of the nozzle and will help direct the flow downstream to the nozzle exit.

Design #3

The final arcjet thruster design is similar to Design 2 in that the argon gas is not directly injected into the cathode. Instead of injecting the gas into the housing perpendicular to the cathode, this design has the argon gas being injected into the housing at an angle. The reason for injecting the argon gas at angle is to create a convective flow of the argon gas that will help cool the cathode by creating a boundary layer. The CAD model of this design is shown in Figure 3.

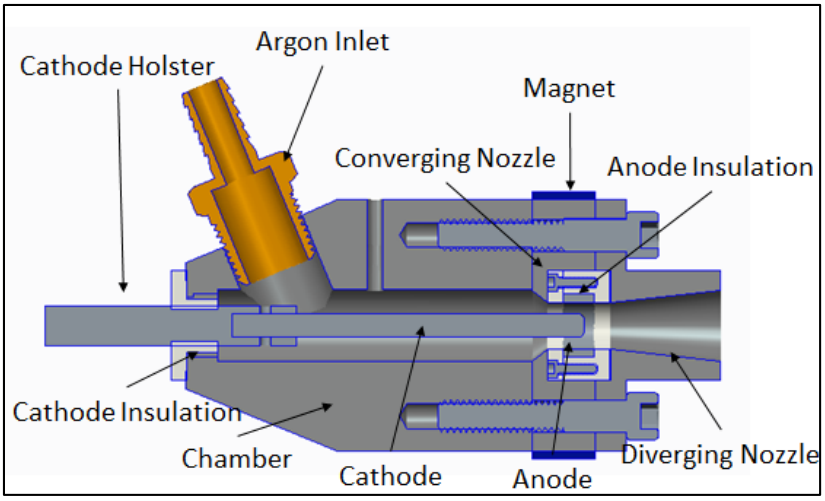

Figure 3: Final Mechanical Design

This design utilizes a cylindrical housing with the end of it acting as the converging portion of the converging diverging nozzle. The long cylindrical rod that is located along the centerline axis of the cylindrical housing is the cathode. The hole on the front side of the housing near the entrance of the cathode is angled in order to allow for the argon gas to be pumped into the housing as previously discussed. The anode is located at the end of the cylindrical housing inside the throat of the converging diverging nozzle. This will ensure that the arc between the cathode and anode will be generated when the argon gas is choked to sonic velocity. After the arc is produced the argon gas becomes ionized and is accelerated past sonic velocity. The argon ions are able to accelerate by increasing the area of the nozzle shown in Fig. 3 in the diverging portion. In order to attach the housing, a flange is incorporated into the design of the diverging nozzle. This will allow for ease of mating and securing the three parts together with the use of screws.

4.2.2 Electrical

Circuit

When the thruster is constructed, the actual anode/cathode spacing and pressure of argon isn't accurately known. Since the breakdown voltage depends on the product of the pressure and anode/cathode distance, it is desired we design a circuit that can adjust the breakdown voltage to match the product of the pressure and distance. There are three different designs we could use to implement these requirements. The first design would be a power processing unit that converts the voltage and current to the proper value for thruster operation. The sponsor specifically asked us to replace this to make the system more efficient so that rules out that option. Another possible design is to create a voltage spike with a capacitive circuit, but the voltage across a capacitor does not change instantaneously, so that would be difficult to do. A better design is to use an inductive circuit to create a voltage spike because the current through an inductor does not change

instantaneously, however the voltage can. This is given by V = L$\frac{di}{dt}$, where di is the change in current, dt is the time it takes for the circuit to open, L is the inductance, and V is the voltage across the inductor. A functional schematic is shown in Figure 4. A potentiometer in place of R_2 is capable of adjusting the voltage spike, because steady state current will drop to zero in the amount of time it takes the insulated gate bipolar transistor (IGBT) to open, thus a potentiometer could control the di term, which controls the voltage spike.

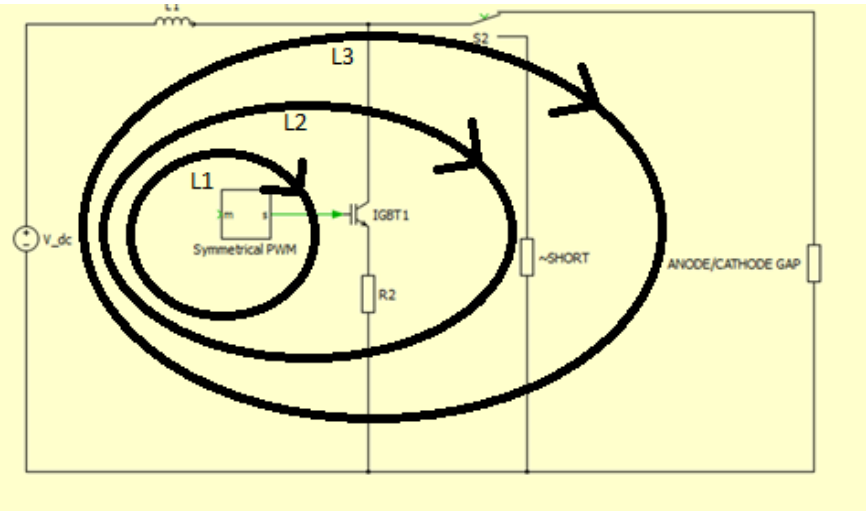

Figure 4: KVL Analysis of Circuit

In order to start up the thruster, the IGBT in Fig. 4, will be closed by a simple selector switch that provides enough voltage to close the IGBT. When the IGBT is closed, loop L1 will conduct current, while loop L2 and L3 will be open circuits. The time it takes L1 to reach steady state is given by, $5 \times \tau = 5 \times \frac{L}{R2}$. We plan to use a potentiometer for R2 that ranges from 14Ω to 105Ω, and inductance of 47 µH, thus τ ranges from 0.448 µs to 3.36 µs. When loop L1 reaches steady state the current will be $I_1 = \frac{V_{dc}}{R2}$, where V_{dc} is the voltage supply from the solar panel, thus I_1 will range from 0.733 A to 5.5 A. When the selector switch is opened the IGBT will open, hence every loop in Fig. 7 will be open, but the inductor will react strongly because the current through an inductor doesn't change instantaneously given by, $= L\frac{di}{dt}$, where dt is the IGBT flip time approximately 250 ns, L = 47 µH, di = I_1 – 0. Therefore, V will range from 137 V to 1.034 kV. This breakdown voltage will create an arc across the anode/cathode gap shown in loop L3, which ionizes the argon flowing through the gap and produces a plasma. Immediately after the arc, current will flow through the plasma, which will act as a resistance that is thought to be very small, hence current will flow through the ~SHORT resistor shown in Fig. 4, loop L2.

Magnets

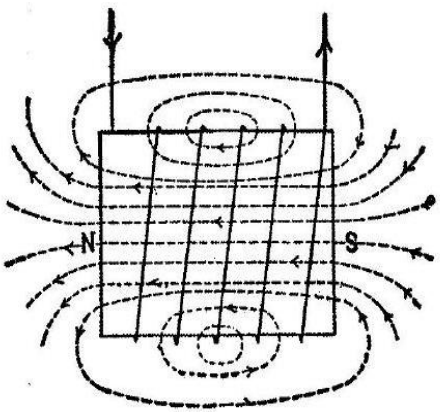

Figure 5: Polarity and Lines of Force in a Magnet

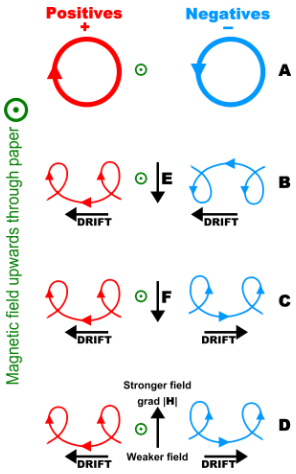

Figure 6: Magnet-Ion Interaction

The magnet will be placed around the nozzle in order to keep the plasma off the walls of the nozzle and will confine the plasma to a certain radius. It also helps increase thrust. Figure 5 depicts an electro-magnet that can be replaced by a bar magnet with the same characteristics. One could imagine a plume of positive and negative charges due to the ionization of argon through the anode/cathode. This plume wants to expand outward but the magnet is pushing the charges of the plume inward causing the charges to move in a helical path as shown in Figure 6. The magnetic field at which we can confine the negative and positive charges in a bar magnet is given by $B = \frac{mv}{qr}$, where m is mass, v is velocity, q is charge, r is radius, and B is the magnetic field. For now we approximate the strength of the magnet to be B = 1 mT, but we must further research the velocity of the charges to get an accurate calculation.

4.3 Evaluation of Designs

Table 1: Decision Matrix

		Design 1		Design 2		Design 3	
	Weights	Rating	Weighted Score	Rating	Weighted Score	Rating	Weighted Score
Life Expectancy	0.1	7.0	0.7	7.0	0.7	8.0	0.8
Material Cost	0.1	2.0	0.2	7.0	0.7	8.0	0.8
Ease of Assembly	0.1	6.0	0.6	8.0	0.8	3.0	0.3
Manufacturability	0.2	5.0	1.0	4.0	0.8	7.0	1.4
Ease of Closing Circuit	0.1	9.0	0.9	9.0	0.9	4.0	0.4
Temperature	0.1	8.0	0.8	4.0	0.4	9.0	0.9
Magnet Insertion	0.1	6.0	0.6	6.0	0.6	8.0	0.8
Gas Insertion	0.1	3.0	0.3	3.0	0.3	9.0	0.9
Reliability	0.1	2.0	0.2	7.0	0.7	8.0	0.8
TOTAL	1.00		5.3		5.9		7.1
RANK			**3**		**2**		**1**

The detailed matrix chart, shown in Table 1, was used as an aid in deciding which design best suited the needs of the project. Each design was measured in its ability to fulfill a total of nine different categories: life expectancy, material cost, ease of assembly, manufacturability, ease of closing the circuit, temperature, magnet insertion, gas insertion and reliability. These categories were given a weight based on the influential importance each would have on the desired final product – the sum of all categories adding up to 1, such that a weighted score could be assigned to each design. Based on the ratings given to each design, a final weighed score is established such that the higher the final total, the more desirable the design.

Designs 1 and 2 fell short for a variety of reasons. Design 1 scored low in reliability since the flow of fuel through the arc isn't maximized as it is in the other two designs. The cost of the first design is also significantly higher due to the selection of an expensive insulation material to be used between the cathode and the grounded material.

As a result of this decision matrix, Design 3 was determined to be the best option. It scored the highest in seven of the nine categories, falling short in its ease of assembly and ease of closing the circuit. This design calls for the magnet to be placed in the throat of the system, as opposed to being wrapped around the exterior of the nozzle. Thus, accurately assembling this design would be qualitatively more difficult. In addition, closing the circuit for this design would be complicated due to the position of the anode within the system.

Conversely, this design scored very high in gas insertion method and temperature control. Design 1 injects the fuel in a direction parallel to the desired thrust direction, Design 2 injects the fuel in a perpendicular direction to the cathode, while Design 3 deposits the fuel at an angle to the final flow direction. This creates swirls aiding in cooling the high temperature fuel and potentially exposing a higher percentage of gas to the electric arc.

4.4 Final Design

The final thruster design was chosen to be Design 3 for reasons stated in the above decision matrix. Figure 7, below, represents the overall testing apparatus setup. As seen in the figure, a large bell jar is to be placed over the thruster and test stand, on top of a baseplate. Seen in the

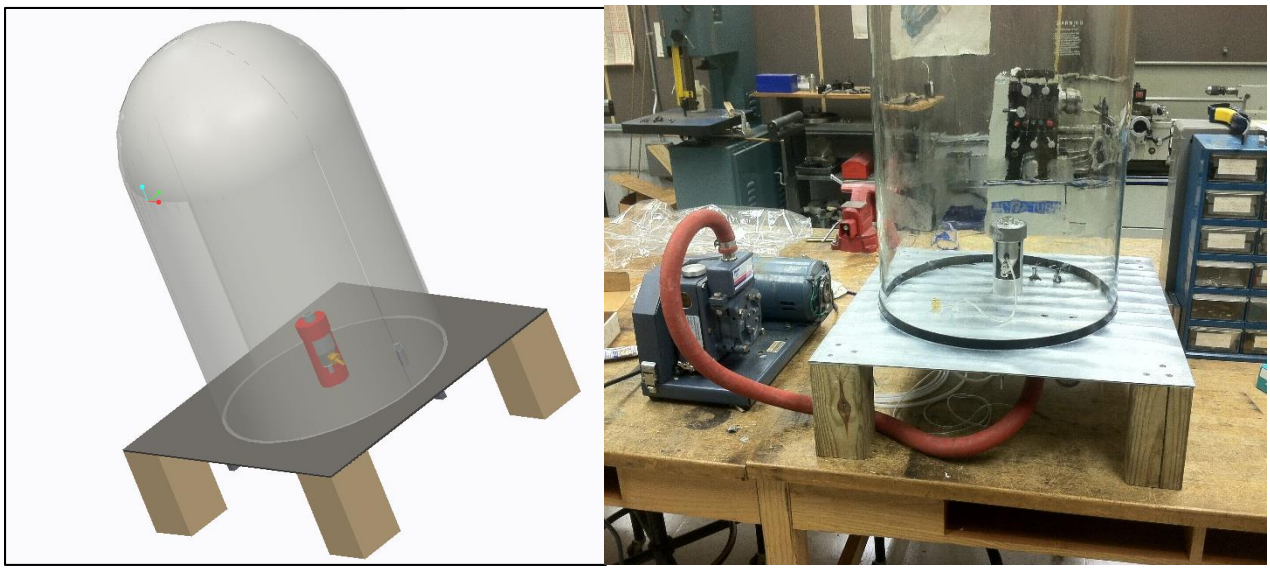

Figure 7: CAD drawing next to actual model

physical model are the wires and tubes connecting the design to an argon gas feed, pressure transducer, vacuum gage, and vacuum pump.

Figure 8 shows the thruster positioned inside of the test stand. The test stand utilizes the existing bolt-hole pattern in the thruster to mount itself vertically. This was designed as such to give maximum clearance between the nozzle exit and the glass bell jar. Exit temperatures have the potential to be very hot and could damage the bell jar if placed in close enough proximity. Additionally, the material trimmed away from the sides of the test stand allow for easy access to the argon and pressure ports. This also reduces the weight of the overall testing apparatus, which is important when selecting an appropriate load cell.

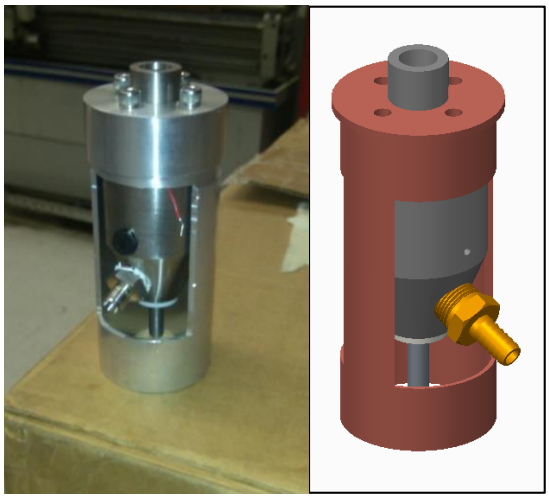

Figure 8: Thruster fixed to test stand

Figure 9 depicts the circuit that was used with the thruster to produce a voltage spike, and after breakdown of argon gas, conduct current through the anode/cathode. A lab power supply was used to replace the 80 volt source (which are the ratings from the solar panels specified by the sponsor), an oscilloscope was used at probe1, and an ammeter at XMM1. As we iterated through testing the thruster varied the potentiometer, which had leads fed through the baseplate along with the oscilloscope, switching mechanism, and power supply.

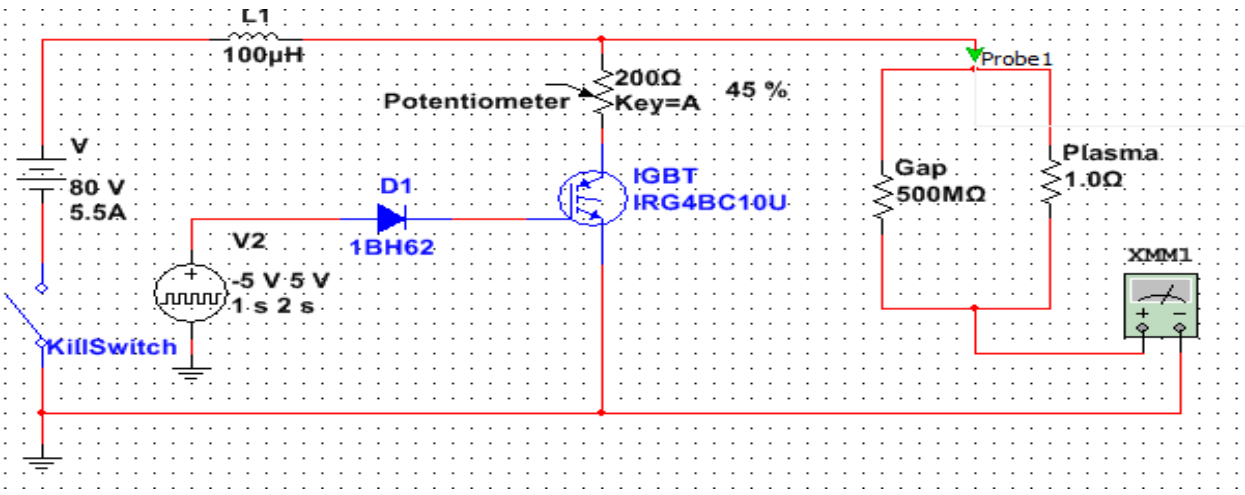

Figure 9: Final Circuit Design

Figure 10 is the final magnet design we decided, which is a flexible magnet. This magnet was easy to wrap around the test stand of the thruster, but still maintained a good magnetic field of roughly 30 mT. Other research papers suggested between 30 and 70 mT, and our sponsor advised us that any magnetic field should help.

Figure 10: Final Magnet Design

5.0 Testing and Analysis Details

Circuit testing revealed promising results with low voltage inputs. The current was limited by the capacity of the bread board since the PCB manufacturing process was unavailable. With a current input of 2 A, a 350V spike (see Figure 11) was achieved but no arc was ignited. Some complications experienced during testing involved finding an appropriate power supply, realizing the resistors were shorted across the baseplate, and clutter due to inability to acquire PCB.

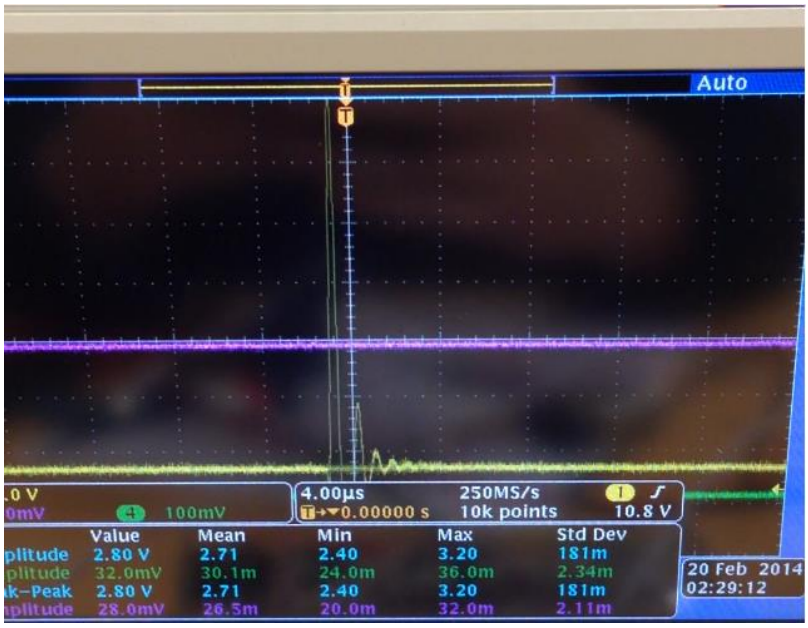

Figure 11: Voltage spike

Initial vacuum chamber testing was performed in the Mechanical Engineering Machine Shop. For these tests, we utilized a Welch 1400 duo-seal vacuum pump. The specifications for this pump noted a capability of 0.1 mTorr. During testing, however, the dial vacuum gauge affixed to the bottom of the baseplate read only -95kPa, 6kPa absolute. It was determined from sponsor input that this vacuum was much too high to achieve breakdown of air/gas mixture. This led us in search of another vacuum pump.

Final testing was performed at the National High Magnetic Field Laboratory in the cryogenics lab. Access to this facility was granted by Dr. Guo and his students Alex Marakov and Jian Gao. Complications with our vacuum gauge led us to believe our vacuum levels were inadequate – this was untrue but prompted us to test with the house vacuum pump at the cryogenics lab. This limited the available gas to use for ionization, and as such, helium was used for testing although all calculations were done using argon. There was a 20-30V breakdown spike difference using helium instead of argon that was accounted for in the electrical circuit.

Figure 12: Final setup of testing apparatus

Figure 12 shows the experimental setup used. Inside the bell jar are all of the circuit components, thruster, test stand, and magnet. Also shown in the picture is the faulty gauge underneath the baseplate, and the more accurate pressure gauge to the left of the baseplate. A proper vacuum seal was attained using vacuum grease underneath the bell jar gasket. Helium was injected through the baseplate into the thruster chamber at a pressure of approximately 500 Pa after the bell jar was evacuated. No visible arc was witnessed at the throat of the nozzle when viewed from above the bell jar. Testing took approximately 30 minutes once properly set up.

6.0 Design for Manufacturing, Reliability and Cost

6.1 Manufacturing Considerations Taken

Many factors play into the design of an engineered prototype. One of the most important factors to be considered is the manufacturability of the design. A good design is good only if it can be made easily, reliably, and timely. This factor was taken into account when designing the Solar Powered Arc Jet Thruster. The design of each component was carefully thought out before submission to the machine shop for manufacture. The processing of the materials was never much of an issue since the main materials for the thruster are metals, namely stainless steel and tungsten. There are two ceramic parts, but a special type of machinable ceramic was chosen to fill the role of the insulator.

From the original design created for the thruster, the following considerations were made:

- The nozzle was shortened to reduce material costs while still maintaining proper area ratio
- Anode insulation was split into two parts to easily replace a defective anode
- Cathode insertion design created for adjustment allowing for varying distance between anode and cathode

- Cathode insulation was threaded to ensure an air-tight seal between chamber and cathode while providing a proper ground for the charged cathode
- Initial chamber inner diameter modified to accommodate large drill bit and to avoid using long boring bar
- Used a standard 2” diameter pipe for ease of machining for test stand
- Standard size holes were chosen to eliminate unnecessary budget allocation for custom machining tools

6.2 Material Selection

- Machinable stainless steel used for nozzle, chamber and throat sections. This also allowed for an increase in thermal mass, which helps to safeguard against adverse heat effects on the thruster.
- Macor insulation was chosen based on its machinability and capacity to withstand high temperatures
- Avoid machining of tungsten by securing cathode in a stainless steel holster

6.3 Machining Work

- Work done by Jeremey Phillips and James Gillman in the COE machine shop
- Guidance and advice given
- Cost effective / time tradeoff

6.4 Bill of Materials

The bill of materials can be seen in Table 1. The parts are referenced in accordance with the assembly in Fig. 13.

Table 1. Bill of Materials

Bill of Materials	
Balloon Number	Name
1	Cathode Holster
2	Cathode
3	Argon Fitting
4	Chamber
5	Converging Nozzle
6	Anode Insulation Screws
7	Anode Insulation Cap
8	Anode
9	Anode Insulation
10	Diverging Nozzle
11	1/4-20 Screws

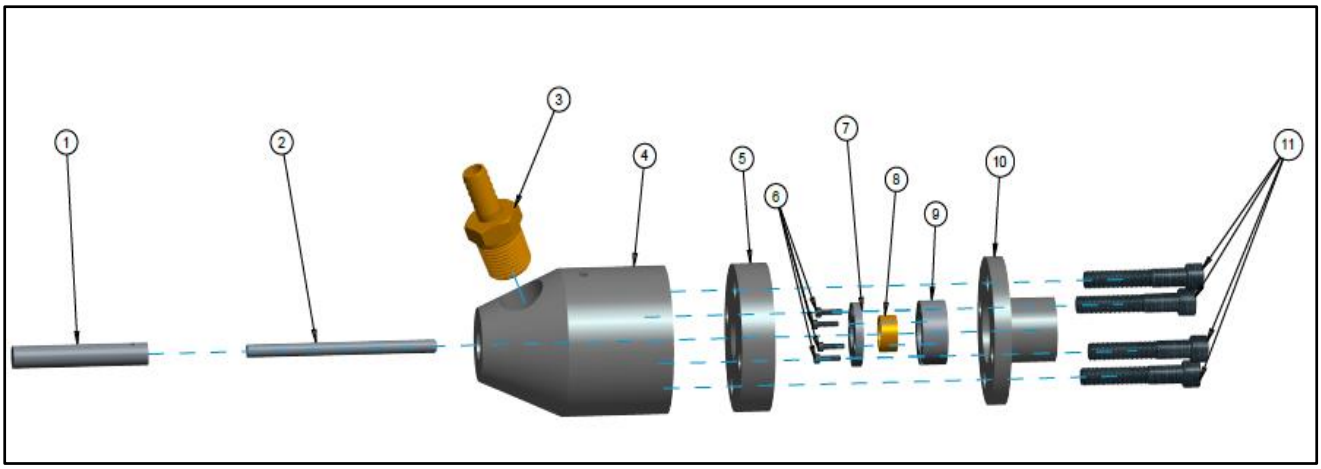

Figure 13: Exploded view of thruster

6.5 Design Changes and Issues

Some issues arose when attempting to assemble the subcomponents of the thruster. One of the issues was the depth of the recess in the anode insulation. The recess was not deep enough to allow the anode piece to be inserted flush into it and capped with the other Macor piece. To avoid machining the ceramic again, the anode was turned down slightly to the proper fit.

Another problem that was encountered was improper fit up of the test stand and cap. The dimensions on the McMaster drawing online were taken to be representative of the physical part that was received, which turned out to be a bad assumption. The ID of the cap and the OD of the pipe needed to be turned down to ensure proper fit.

When assembling the thruster the Macor cap was cracked when it was tightened onto the anode and corresponding Macor piece. This occurred because the wire inserted into the slot had too large of a diameter. This caused stresses on the groove and initiated a crack. A new piece was manufactured and will be used as a backup.

6.6 Design for Reliability

Certain pieces of the thruster are more susceptible to failure than others. In this design the pieces most likely to fail are the cathode and anode. This is because both are exposed to extremely high voltages and temperatures. This being the case, spare parts have been provided in the event of melting. The stainless steel chamber and body of the thruster are extremely durable and provide a very high thermal mass, which is important in space application.

The circuit is simple and reliable, but still needs to be integrated into a PCB. The only energy losses are due to the plasma once the thruster is operating, optimizing the energy from the solar panels and reducing energy losses due to the PPU. Flexible permanent magnets are used for ease of assembling to the thruster, and are reliable in space for long periods of time.

7.0 Marketing

The project and apparatus at hand is not a marketable product. The scope of this project was more of a research and development task; not a design for production, consumers or aerospace companies.

8.0 Considerations for Environment, Safety and Ethics

Some safety issues associated with arcjet thrusters are, if not fully knowledgeable on the subject, one could severely injure or possibly kill themselves. The thruster produces high voltage which can be extremely harmful, especially if it travels across your heart. Another safety issue is asphyxiation from argon while testing. The heat produced by the thruster could potentially melt the glass bell jar. An issue thought to be of concern last semester was the amount of vacuum the bell jar could withstand. It was thought that the bell jar could potentially implode, which introduced a slew of safety concerns. After testing, however, it was realized that the bell jar was plenty capable of withstanding the vacuum pressure inside it.

9.0 Communications

Our team communicates effectively with each other, our advisors, and sponsor. We make the most of our meeting times and are efficient with our meetings. We set up meetings and conference calls with our advisors and sponsor about every two weeks. Our group meets once to twice a week depending on the work load and requirements of the project. We use email, text messaging, twitter, and phone calls to communicate information about project deadlines and plans.

10.0 Conclusions

Elimination of the power processing unit as demonstrated in our choice of Design 3 would, theoretically, allow for sufficient thrust at a reduced cost for spacecraft propulsion. In addition, lifetime of the system is increased since failure of PPU is no longer in consideration. Price of the general design is also significantly diminished by using direct-drive, as current designs must allocate a large portion of the budget to invest in a power processing unit. The design chosen should effectively capture the opportunity to both provide thrust with magnetic acceleration of ionized particles and thermal expansion of argon gas and plasma.

As mentioned above, a major expenditure for the project is derived from the need to manufacture a vacuum chamber specifically for testing purposes. Had this design been implemented and tested in a facility already possessing a viable vacuum chamber, the costs of this project would be greatly reduced. Taking this into account, the overall expenses for a design such as this provides a better opportunity to meet the customer's budget of $500.

Thankfully, expensive components related to the vacuum chamber were borrowed, relieving some strain associated with staying within the budget. The difficulty in manufacturing the vacuum chamber, however, succeeded in extending the depth of this project. Designing a vacuum chamber was not specifically requested by the sponsor, yet comprised a large portion of the time and efforts provided by the team.

Even with this challenge, three of the main objectives of this project were still accomplished: the vacuum worked with no detectible leaks, the circuit performed above expectations, and a scalable arcjet thruster was manufactured. Time constraints and equipment availability became an issue, as the vacuum chamber took longer than expected to construct. Had there been more time available for testing, the requirements of this project would have been confidently achieved. Recommendations for what would be accomplished, had there been more time, are detailed below.

11.0 Recommendations for Future Work

As mentioned above, a large hurdle in completing all sponsor requirements was obtaining a viable vacuum. Were there more time left in the semester, more testing would be possible to validate all aspects of the project. In order to better test breakdown inside the vacuum, air should be vacuumed out of the bell jar, flooded with argon gas, and then vacuumed back down to theoretical throat pressure levels. Once ability to breakdown gas is verified, more data could be collected on minimum breakdown voltage and pressure at the throat.

Additionally, a more precise vacuum gauge would be required to more accurately control pressure values. Testing would have been easier had we known about the plasma laboratory owned by the chemistry department. This lab had access to argon and the necessary power source, which would have reduced the need to transport all equipment across buildings. Furthermore, experienced graduate students could have been another source for advice in testing with plasma.

Future work could also be done on improving data acquisition. Measurements for thrust, housing temperature, voltage spikes and thruster chamber pressure would be ideal. These could each be carried out with a load cell, thermocouple, differential voltage probes, and differential pressure transducer respectively. These measurements could more accurately plot the required voltage and throat pressure to achieve breakdown for multiple gases.

12.0 Schedule, Resources and Budget

12.1 Gantt Chart Scheduling

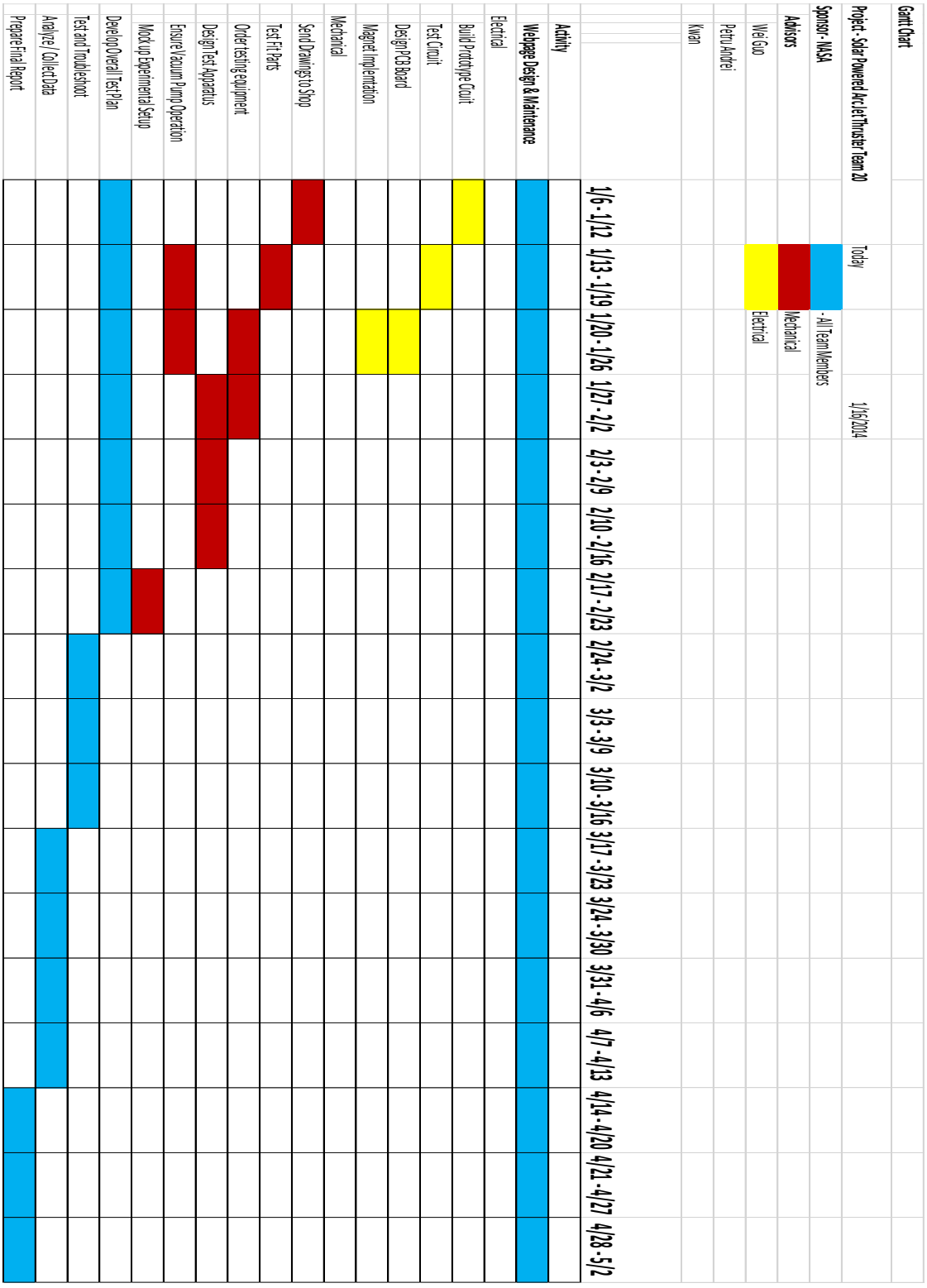

12.2 Budget

Table 2: Budget Analysis for Design 3

Component	Description	Quantity	Cost	Manufacturer
Cathode	Tungsten Rod, 3/16" x 6" P#8788A153	2	$ 33.24	McMaster Carr
	Stainless Steel 303, 3/16" x 6' P#8984K93	1	$ 7.77	McMaster Carr
Anode	SS Steel Tube 1/2 OD, 0.37 ID 3' P# 9220K461	1	$ 8.79	McMaster Carr
Hose Fitting from Baseplate Fitting	3/8" Threaded Female Hose Fitting P# 5346K85	1	$ 11.00	McMaster Carr
Vacuum Gauge	Bottom Connection Vacuum Gauge P#4004K62	1	$ 10.61	McMaster Carr
Vacuum Grease	High-Vacuum Grease 5.3 oz. P#2966K52	1	$ 26.68	McMaster Carr
Argon Hose	3/8" ID x 5' Hose P#5304K24	1	$ 6.10	McMaster Carr
Threaded Pipe Nipple	P#44615K462	2	$ 3.24	McMaster Carr
Vacuum Hose Fitting 90 deg	P#5346K125	1	$ 10.20	McMaster Carr
Coupling for Vacuum Gauge	P#4429K111	1	$ 5.70	McMaster Carr
Mounting Pipe	2.375" OD, 2.157" ID X 12" P# 4561T611	1	$ 22.58	McMaster Carr
Housing/Nozzle	Stainless Steel 303, 2' Diameter, Stock P#8984K573	1	$ 79.64	McMaster Carr
Gasket	All Purpose Sheet Gasket 6"x6" P# 9470K26	2	$ 6.02	McMaster Carr
Bolts (Anode)	P# 92185A078	1	$ 3.23	McMaster Carr
Mating Bolts	P# 92185A546	1	$ 5.43	McMaster Carr
Nuts for Mating Bolts	P# 91845A029	1	$ 4.57	McMaster Carr
Insulation	Macor Rod P#8489K81	1	$ 72.95	McMaster Carr
IGBT	P#IRG7PH30K10DPBF	1	$ 8.73	Digi-Key
Inductor	100.0 µH, 6 A P#1410460C	1	$ 2.62	Digi-Key
Switch	P#C3900BA	2	$ 8.92	Digi-Key
Potentiometer	P#AVT20020E200R0KE	2	$ 31.24	Digi-Key
Flexible Magnet	12"x2" P# 3651K3	1	$ 51.20	American Science & Surplus
		TOTAL	**$ 420.46**	
	Remaining Budget		$ 79.54	

Due to the fact that this project is federally funded through NASA, the budget provided was limited to $500. As shown in Table 2, the remaining budget is enough to allow for any unforeseen complications. It should be noted, however, that this budget corresponds to a small-scale thruster – increasing its size for actual implementation on a satellite will drive up the cost tremendously.

12.3 Resources

Many different mechanical and electrical resources were utilized, including:

- Oscilloscope
- Power supply
- Multimeter
- Polyflow tubing
- Bell jar
- Baseplate
- Vacuum pump
- Gas feed
- Machining advice
- Simulation tools

13.0 References

1) Polzin, Kurt. "Senior Design Project Definition." NASA, n.d. Web. 26 Sept. 2013.
2) Matthew Krolak. “MPD Thruster Thesis.” Worcester Polytechnic Institute, May 2007.
3) Nicolas Augustus Rongione. “Direct Solar Powered Arcjet Thruster (DiSPAT)” NASA, n.d. August 9, 2013.
4) William Anthony Hargus, Jr. “Hall Acceleration Mechanism” US Air Force Research Laboratory. March 2001
5) Geoff Dickinson. “Non-impulsive orbit raising using an ATOS type arcjet thruster” ASEN5050. Dec. 2002.
6) F. Paganucci, P. Rossetti, M. Andrenucci. “Performance of an Applied Field MPD Thruster” RIAME-MAI. 2001.

14.0 Appendix

14.1 Designed Component Details and Specs

14.1.1 Mechanical

Design #3

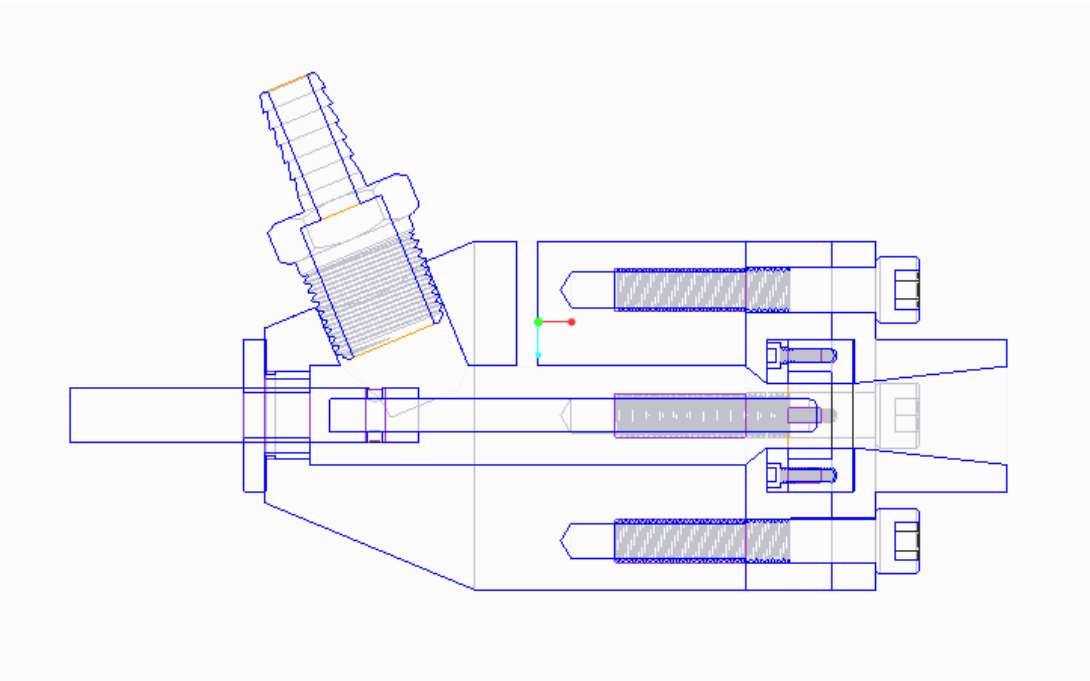

Figure 14

*Above is a rough schematic of the design to be used, however the exact dimensions have not been chosen yet.

14.1.2 Electrical

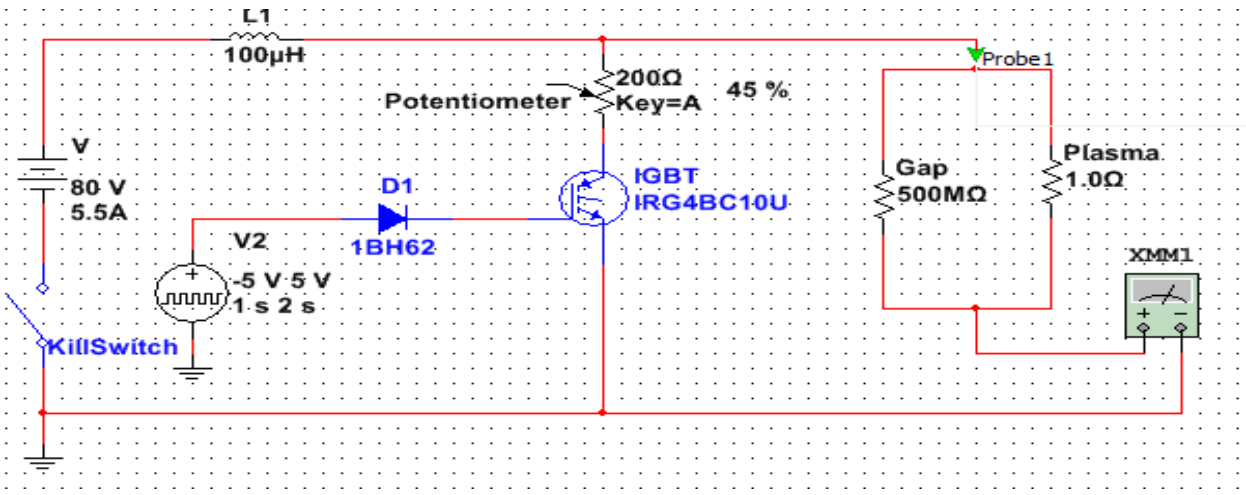

Figure 15

Figure 15 is a detailed design of a functional circuit that meets the requirements. The magnet design will look similar to fig. 8.

14.2 Detailed Analysis, Computations

14.2.1 Mechanical

Feed Calculations for NASA Direct-Drive Solar Powered Arcjet Thruster

$P_{vacuum} := 0.5Pa$

$P_{Chamber} := 550Pa$

$\rho_{Ar} := 1.784 \frac{kg}{m^3}$ $D_{Cathode} := 0.1875in$

$T_0 := 293.15K$ $T_t := 0.833 \cdot T_0$ $D_{Feed} := 0.375in$

$\gamma := 1.667$ $T_s := .4086 \cdot T_t$

$D_{Throat} := 0.37in$

$R_1 := 287 \frac{J}{kg \cdot K}$ $D_{Exit} := 0.5665in$ $a_{Ar} := \sqrt{\gamma \cdot R_1 \cdot T_0}$

$a_{Ar.exit} := \sqrt{\gamma \cdot R_1 \cdot T_s} = 218.487 \cdot \frac{m}{s}$ $P_{Throat} := 267Pa$ $a_{Ar.t} := \sqrt{\gamma \cdot R_1 \cdot T_t}$

The velocity exiting the throat of the nozzle should be equal to the speed of sound for Argon (before plasma generation). This is under the assumptions that Argon is behaving as an ideal gas and still abides by gas dynamic properties.

$V_{Throat} = a_{Ar}$ $V_{Throat} := a_{Ar.t}$ $A_{Throat} = A_{Throat}(without\_cathode) - A_{Cathode}$

$A_{Cathode} := \frac{\pi}{4} \cdot D_{Cathode}^2 = 0.028 \cdot in^2$ $A_{Exit} := \frac{\pi}{4} \cdot D_{Exit}^2 = 0.252 \cdot in^2$

$A_{Throat} := \frac{\pi}{4} \cdot D_{Throat}^2 - A_{Cathode} = 0.08 \cdot in^2$ $A_{Chamber} := A_{Exit} - A_{Cathode} = 0.224 \cdot in^2$

$dm_{Ar} := \rho_{Ar} \cdot V_{Throat} \cdot A_{Throat} = 0.031 \frac{kg}{s}$ $\frac{A_{Exit}}{A_{Throat}} = 3.154$

Estimating Thrust and Specific Impulse

$M_{exit} := 2.69$ $V_{exit} := M_{exit} \cdot a_{Ar.exit} = 587.73 \frac{m}{s}$ $P_{exit} := P_{Throat} \cdot 0.04362 = 11.647 Pa$

$F_{Thrust} := dm_{Ar} \cdot V_{exit} + (P_{exit} - P_{vacuum}) \cdot A_{Exit} = 18.478 N$

$I_{sp} := \frac{F_{Thrust}}{dm_{Ar} \cdot g} = 59.938 s$

The C-D Nozzle is designed for a Mach # of 2, again this is under the assumption that once the Argon is ionized it will still behave as an ideal gas (Which it will not but gotta start somewhere). However, do to the existence of the cathode placed in the throat of the nozzle will increase the effective area ratio increasing the designed mach number.

$M_{Exit.no\_cathode} = 2$ $M_{Exit.cathode} = 2.69$

Equations/Calculations:

$$A_{Hose} := \frac{\pi \cdot D_{Feed}^{2}}{4} = 0.11 \cdot in^{2}$$

$$P_1 + \frac{1}{2} \cdot \rho_{Ar} \cdot V_1^{2} = P_2 + \frac{1}{2} \cdot \rho_{Ar} \cdot V_2^{2} \quad \text{Eqn: 1}$$

$$dm_{Ar} = \rho_{Ar} \cdot V_{Ar} \cdot A \quad \text{Eqn: 2}$$

$$V_{Hose} := \frac{dm_{Ar}}{\rho_{Ar} \cdot A_{Hose}} = 247.298 \frac{m}{s}$$

$$M_{Hose} := \frac{V_{Hose}}{a_{Ar}} = 0.66$$

If we set the Pressure leaving the Argon Cylinder to be 1psi, and assume that this is the back pressure that the chamber feels and not the 2500psi of the Argon Cylinder.

$P_{Hose} := 1000Pa$

$$V_{Chamber} = \sqrt{2 \cdot \frac{\left[\left(P_{Hose} - P_{Chamber}\right) + \left(\frac{1}{2}\right) \cdot \rho_{Ar} \cdot V_{Hose}^{2}\right]}{\rho_{Ar}}} \quad \text{From Bernoulli's Eqn}$$

$$V_{Chamber} := \sqrt{2 \cdot \frac{\left[\left(P_{Hose} - P_{Chamber}\right) + \left(\frac{1}{2}\right) \cdot \rho_{Ar} \cdot V_{Hose}^{2}\right]}{\rho_{Ar}}} = 248.316 \frac{m}{s}$$

$$M_{Chamber} := \frac{V_{Chamber}}{a_{Ar}} = 0.663$$

$$V_{C\_Ideal} := \frac{dm_{Ar}}{\rho_{Ar} \cdot A_{Chamber}} = 121.695 \frac{m}{s}$$

$$M_{Chamber\_Ideal} := \frac{V_{C\_Ideal}}{a_{Ar}} = 0.325$$

Comsol Calculations:

Calculating number density (n_density) and incident molecular flux, phi, for comsol

$1 \cdot 10^{-4}\,\text{torr} = 0.013\,\text{Pa}$ $\quad L_{Chamber} := 2.5\text{in}$ $\quad t := 10\text{s}$ $\quad M_{Ar} := .039948\,\frac{\text{kg}}{\text{mol}}$

$\text{Vol}_{Chamber} := A_{Chamber} \cdot L_{Chamber} = 9.195 \times 10^{-6}\,\text{m}^3$

$m_{Ar} := dm_{Ar} \cdot t = 0.314\,\text{kg}$

$n := \frac{m_{Ar}}{M_{Ar}} = 7.869\,\text{mol}$ $\quad \text{Avo} := 6.022 \cdot 10^{23}\,\frac{1}{\text{mol}}$

$N_{mol} := n \cdot \text{Avo}$

$n_{density} := \frac{N_{mol}}{\text{Vol}_{Chamber}} = 5.154 \times 10^{29} \cdot \frac{1}{\text{m}^3}$

$\nu := 6925\,\frac{\text{m}}{\text{s}}$

$\Phi_f := \frac{1}{4} \cdot n_{density} \cdot \nu = 8.923 \times 10^{32}\,\frac{1}{\text{m}^2 \cdot \text{s}}$

14.2.2 Electrical

For the magnet we calculated the magnetic field with $B = \frac{mv}{qr}$, $v = \sqrt{\frac{20eV}{3m}}$. These equations simplify to give us B = 2.889/r mT.

As described in section 3.2.2.1, the inductor of figure 11 will be capable of producing a voltage spike of magnitude $V = L\frac{di}{dt}$, where dt = 250 ns, L = 47 µH, di = 5.5_{max} or 0.733_{min} A, thus the breakdown voltage will range from 137 V to 1.034 kV.